



## *p*-Terphenyls from the fruiting bodies of *Paxillus curtisii* and their antioxidant properties

In-Kyoung Lee<sup>a</sup>, Jin-Young Jung<sup>a</sup>, Young-Sook Kim<sup>a</sup>, Man Hee Rhee<sup>b</sup>, Bong-Sik Yun<sup>a,\*</sup>

<sup>a</sup> Division of Biotechnology, College of Environmental and Bioresource Sciences, Chonbuk National University, Ma-dong 194-5, Iksan, Jeonbuk 570-752, Republic of Korea

<sup>b</sup> Laboratory of Veterinary Physiology and Signaling, College of Veterinary Medicine, Kyungpook National University, Daegu 702-701, Republic of Korea

### ARTICLE INFO

#### Article history:

Received 6 March 2009

Revised 24 April 2009

Accepted 25 April 2009

Available online 3 May 2009

#### Keywords:

*p*-Terphenyls

Curtisians

*Paxillus curtisii*

Free radical scavengers

Fenton reaction

### ABSTRACT

New *p*-terphenyls, curtisians R (1)–V (5), have been isolated together with known compounds, curtisians E, I–P, and kynapcin-12, from the methanolic extract of the fruiting bodies of *Paxillus curtisii* (Paxillaceace). Their structures were established by various spectroscopic analyses including 1D- and 2D-NMR experiments, as well as high-resolution FAB-mass analysis. They exhibited significant protective effects against oxidative damage of supercoiled DNA and 2-deoxyribose by hydroxyl radicals generated from the Fenton reaction.

© 2009 Elsevier Ltd. All rights reserved.

## 1. Introduction

The oxidation of biological molecules such as lipids, proteins, and DNA by reactive oxygen is thought to be responsible for the development of numerous pathological processes including cancer, aging, inflammatory disease, and ischemia.<sup>1</sup> Chain-breaking antioxidants such as vitamin E suppress oxidation and protect biological molecules and tissues from oxidative damage.<sup>2,3</sup> As a consequence, the role of antioxidants has received a great deal of attention, with the first trial to investigate antioxidant efficacies designed to assess radical scavenging effects. As part of our ongoing efforts to search for free radical scavengers from the methanolic extracts of wild mushrooms, five new *p*-terphenyl antioxidants, curtisians R (1)–V (5), have been isolated, together with known compounds, curtisians E, I–P, and kynapcin-12, from the methanolic extract of the fruiting bodies of *Paxillus curtisii* (Paxillaceae). This mushroom has strongly corrugated, bright, yellowish gills and grows on the sides or bottoms of rotting logs. It is distinguished by its characteristic smell of cinnamon and is difficult to find given its rarity in nature. In a previous study, we isolated curtisians A–D from the fruiting bodies of *P. curtisii* as free radical scavengers and neuroprotective agents and proposed their modes of action to be iron chelation.<sup>4,5</sup> Recently, curtisians E–Q were reported from Japanese *P. curtisii* as DPPH (1,1-diphenyl-2-picrylhydrazyl) radical scavengers.<sup>6–8</sup> In this study, we describe the

isolation and structure determination of five new *p*-terphenyl antioxidants, curtisians R (1)–V (5) (Fig. 1), and their free radical scavenging activity and protective effects against oxidative damage of supercoiled DNA and 2-deoxyribose by hydroxyl radicals.

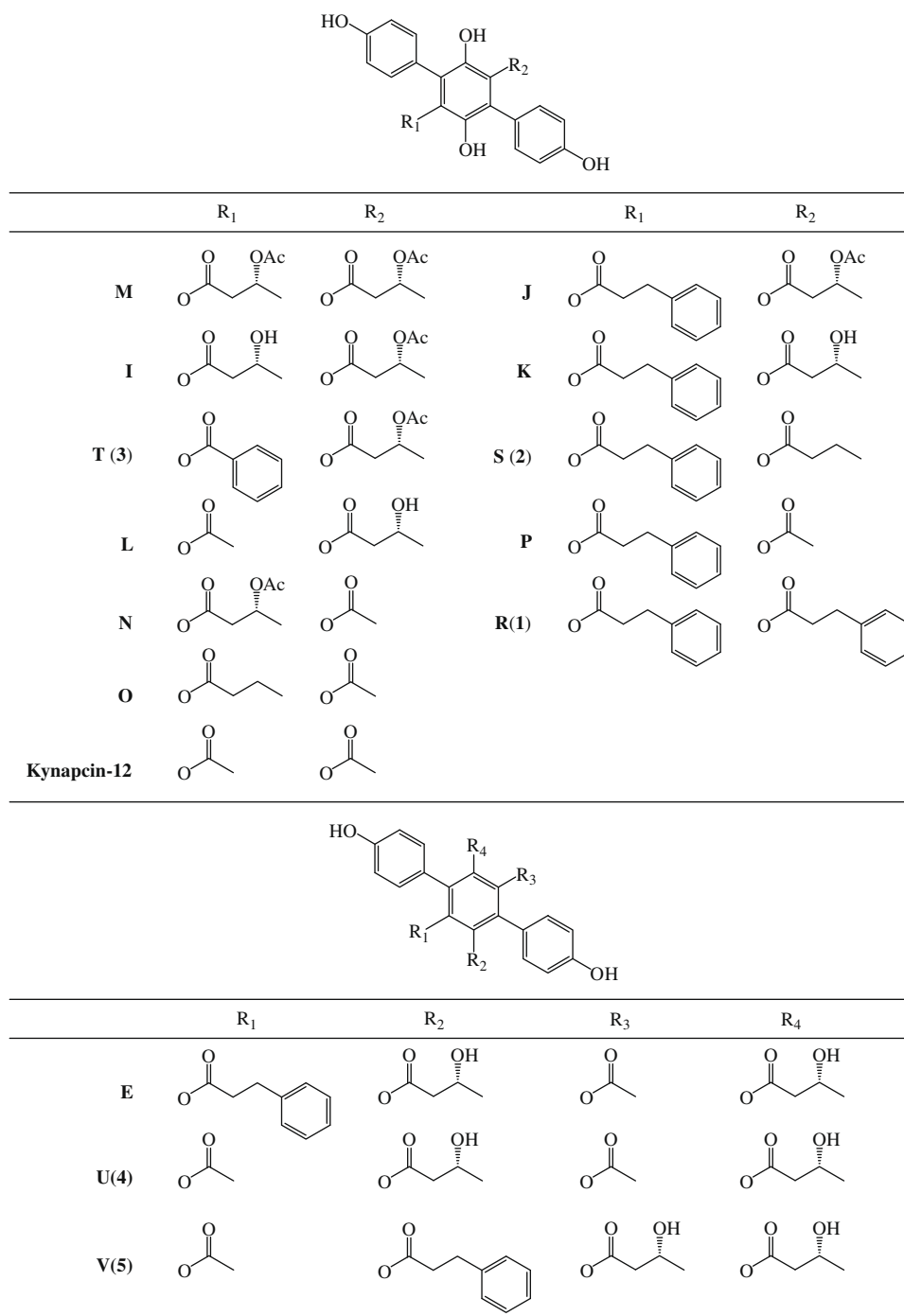
## 2. Structures of curtisians R (1)–V (5)

The methanolic extract of the fruiting bodies of *P. curtisii* was partitioned between ethyl acetate and water. The ethyl acetate-soluble portion was chromatographed on a column of silica gel and eluted with a gradient of increasing methanol (2–50%) in chloroform to afford the antioxidant fraction. The fraction was subjected to a column of Sephadex LH-20, eluted with a mixture of chloroform–methanol (1:1), followed by preparative HPLC using a reversed-phase C<sub>18</sub> column to provide curtisians R (1)–V (5), together with the known compounds, curtisians E, I–P, and kynapcin-12. All compounds isolated had the characteristic smell of cinnamon. Ten of the 15 compounds were identified as curtisians E, I, J, K, L, M, N, O, and P, and kynapcin-12 on the basis of their physicochemical properties and NMR spectral data, which were in good agreement with those published previously.<sup>6–9</sup> Although kynapcin-12 was isolated from *Polyozellus multiplex*,<sup>9,10</sup> it was first reported from the genus *Paxillus*.

Curtisian R (1) was isolated as a dark brown powder, and its molecular formula was determined to be C<sub>36</sub>H<sub>30</sub>O<sub>8</sub> by high resolution FAB-mass (*m/z* 591.2062 [M+H]<sup>+</sup>, Δ + 2.1 mmu). The molecular formula required 22° of unsaturation. The UV absorption

\* Corresponding author. Tel.: +82 63 270 2847; fax: +82 63 850 0834.

E-mail address: [bsyun@chonbuk.ac.kr](mailto:bsyun@chonbuk.ac.kr) (B.-S. Yun).



maximum at 262 nm indicated the presence of an aromatic group, while the IR spectrum suggested the presence of hydroxyl ( $3444\text{ cm}^{-1}$ ) and aromatic ( $1651$ ,  $1560\text{ cm}^{-1}$ ) groups. The  $^1\text{H}$  NMR spectrum of **1** in  $\text{CD}_3\text{OD}$  exhibited five protons in the aromatic region assignable to a phenyl group, four aromatic protons at  $\delta$  7.13 and 6.81 attributable to a 1,4-disubstituted benzene, and four protons at  $\delta$  2.62 and 2.34 from two methylenes. In the  $^{13}\text{C}$  NMR spectrum, 14 carbon peaks were evident with four peaks at  $\delta$  132.7, 129.5, 129.2, and 116.0 significantly higher than others in intensity. These spectral data implied that compound **1** should be a symmetrical structure.<sup>4</sup> A partial structure, phenylpropionyl moiety, was established by the  $^1\text{H}$ – $^1\text{H}$  COSY spectrum, providing correlations for the phenyl group and ethyl moiety, and the HMBC

correlations of ethyl protons to phenyl group and ester carbonyl carbon (Fig. 2). Comparison of the  $^1\text{H}$  and  $^{13}\text{C}$  NMR spectral data of **1** with those of curtisian P, in combination with the molecular formula, indicated that a phenylpropionyl group in **1** replaced the acetoxy group of curtisian P. Thus, the structure of **1** was determined as a new *p*-terphenyl derivative with two para-substituted phenylpropionyl groups on the central aromatic ring.<sup>8</sup>

Curtisian S (**2**) was obtained as a dark brown powder, and its molecular formula of  $\text{C}_{31}\text{H}_{28}\text{O}_8$  was established by high-resolution FAB-mass measurement ( $m/z$  529.1874  $[\text{M}+\text{H}]^+$ ,  $\Delta + 1.1\text{ mmu}$ ). The UV absorption maximum at 262 nm and IR absorption bands at  $3433$ ,  $1650$ , and  $1558\text{ cm}^{-1}$ , very similar to compound **1**, indicated the presence of hydroxyl and aromatic groups. The  $^1\text{H}$  NMR spec-

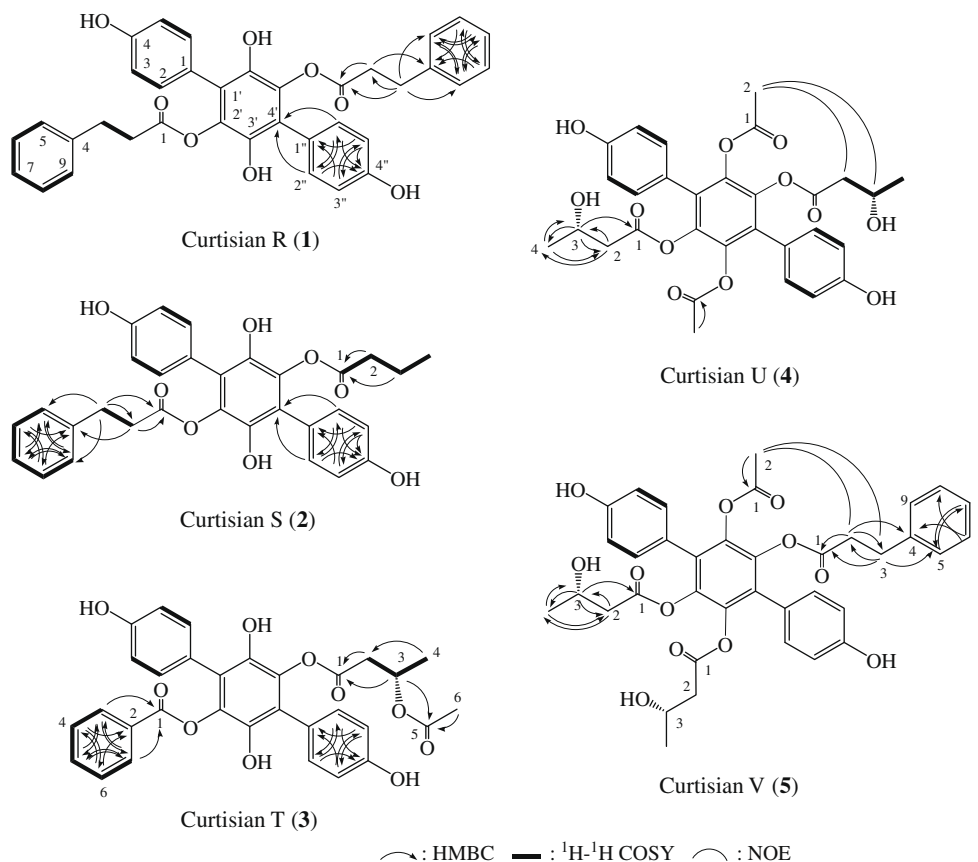


**Figure 1.**  $^1\text{H}$ - $^1\text{H}$  COSY and HMBC correlations for curtisians R (1)–V (5) and key NOESY correlations for curtisians U (4) and V (5).

trum showed signals assignable to two 1,4-disubstituted benzenes, a phenylpropionyl group, and a *n*-butryl group, all supported by HMBC correlations, as shown in Figure 2. The  $^1\text{H}$  and  $^{13}\text{C}$  NMR spectra of **2** resembled those of **1**, except for the presence of a *n*-butryl group instead of the phenylpropionyl group in **1**. Therefore, the structure of **2** was determined to be a new *p*-terphenyl derivative with two hydroxyl, one *n*-butryl, and one phenylpropionyl substituents on the central ring, as shown in Figure 1.

Curtisian T (**3**) was obtained as a dark brown powder, and its molecular formula of  $\text{C}_{31}\text{H}_{26}\text{O}_{10}$  was established by high resolution FAB-mass spectrometry ( $m/z$  559.1567  $[\text{M}+\text{H}]^+$ ,  $\Delta$  = 3.7 mmu). The UV absorption maxima at 263 and 230 nm and IR absorption bands

at 3421, 1716, 1651, and  $1558\text{ cm}^{-1}$  indicated the presence of hydroxyl, ester carbonyl, and aromatic groups. Interpretation of  $^1\text{H}$ - $^1\text{H}$  COSY and HMBC spectral data of **3**, along with  $^1\text{H}$  and  $^{13}\text{C}$  NMR data, suggested the presence of a 3-acetoxybutyryl group ( $\delta_{\text{H}}$  0.90, 1.77, 2.39, 4.91;  $\delta_{\text{C}}$  19.5, 20.9, 40.5, 68.0, 169.9, 171.9) and benzoyl group ( $\delta_{\text{H}}$  7.42, 7.58, 7.88;  $\delta_{\text{C}}$  129.7, 130.2, 130.9, 134.8, 166.1) in **3** (Fig. 2). A partial structure, 3-acetoxybutyryl moiety, was secured by:  $^1\text{H}$ - $^1\text{H}$  COSY correlations between H-2 to H-4; HMBC correlations of H-2 of 3-acetoxybutyryl to its carbonyl carbon (C-1) and of H-3 to the carbonyl carbon of acetyl group. The benzoyl group was confirmed by long-range correlations of H-3 and H-7 to its C-1, as shown in Figure 2. These results

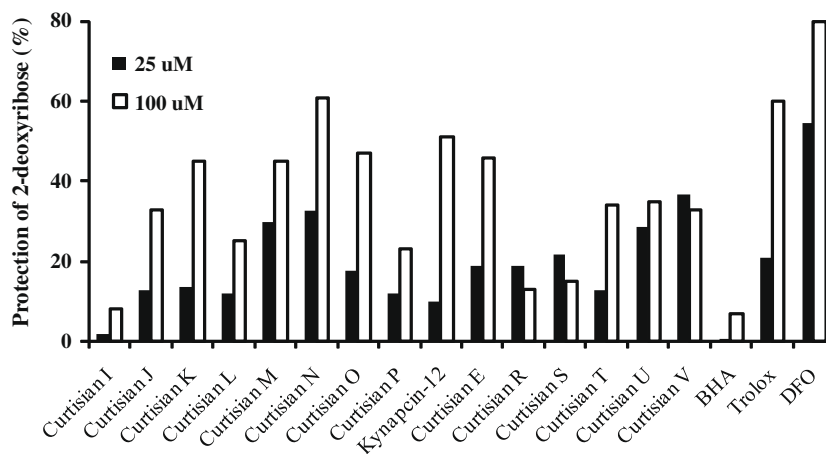


**Figure 2.** Hydroxyl radical scavenging activities of curtisians, trolox, BHA, and DFO on the oxidative degradation of 2-deoxyribose induced by ferrous and hydrogen peroxide.

**Table 1**<sup>1</sup>H and <sup>13</sup>C NMR spectral data for compounds **1–3** in CD<sub>3</sub>OD

No.	1		2		3	
	$\delta_C$	$\delta_H$	$\delta_C$	$\delta_H$	$\delta_C$	$\delta_H$
1,1''	124.9		124.9, 125.0		124.8, 124.9	
2,6,2'',6''	132.7	7.13 (d, $J = 8.4$ ) <sup>a</sup>	132.6, 132.7	7.14, 7.15 (d, $J = 8.4$ )	132.6, 132.7	7.20, 7.22 (d, $J = 8.8$ )
3,5,3'',5''	116.0	6.81 (d, $J = 8.4$ )	115.9, 116.0	6.81, 6.83 (d, $J = 8.4$ )	116.0, 116.1	6.73, 6.84 (d, $J = 8.8$ )
4,4''	158.1		158.2		158.0, 158.2	
1',4'	123.9		123.8, 123.9		123.9, 124.0	
2',5'	134.8		134.7, 134.8		134.7, 134.8	
3',6'	142.5		142.4, 142.5		142.6, 142.7	
1a	172.4		172.5		166.1	
2a	36.1	2.34 (d, $J = 7.4$ )	36.1	2.49 (d, $J = 7.4$ )	130.2	
3a	31.3	2.62 (d, $J = 7.4$ )	31.3	2.69 (d, $J = 7.4$ )	130.9	7.88 (d, $J = 7.6$ )
4a	141.6		141.7		129.7	7.42 (br, t, $J = 7.6$ )
5a	129.2	7.02 (br, d, $J = 7.2$ )	129.4	7.06 (br, d, $J = 6.8$ )	134.8	7.58 (br, t, $J = 7.6$ )
6a	129.5	7.19 (br, t, $J = 7.2$ )	129.5	7.22 (br, t, $J = 6.8$ )	129.7	7.42 (br, t, $J = 7.6$ )
7a	127.2	7.09 (br, t, $J = 7.2$ )	127.2	7.21 (br, t, $J = 6.8$ )	130.9	7.88 (d, $J = 7.6$ )
8a	129.5	7.19 (br, t, $J = 7.2$ )	129.5	7.22 (br, t, $J = 6.8$ )		
9a	129.2	7.02 (br, d, $J = 7.2$ )	129.4	7.06 (br, d, $J = 6.8$ )		
1b	172.4		173.1		169.9	
2b	36.1	2.34 (d, $J = 7.4$ )	36.2	2.00 (t, $J = 7.2$ )	40.5	2.39, 2.20 (dd, $J = 16.4, 7.2$ )
3b	31.3	2.62 (d, $J = 7.4$ )	19.1	1.35 (m, $J = 7.2$ )	68.0	4.91 (m)
4b	141.6		13.4	0.71 (t, $J = 7.2$ )	19.5	0.90 (d, $J = 6.4$ )
5b	129.2	7.02 (d, $J = 7.2$ )				
6b	129.5	7.19 (br, t, $J = 7.2$ )				
7b	127.2	7.09 (br, t, $J = 7.2$ )				
8b	129.5	7.19 (br, t, $J = 7.2$ )				
9b	129.2	7.02 (d, $J = 7.2$ )				
3b-Ac					20.9, 171.9	1.77 (s)

All spectra were recorded at 400 MHz for proton and at 100 MHz for carbon.

<sup>a</sup> Proton resonance multiplicity and coupling constant ( $J = \text{Hz}$ ) in parenthesis.

established the structure of **3** as a new *p*-terphenyl derivative with two hydroxyl, one 3-acetoxybutyryl, and one benzoyl substituent on the central aromatic ring.

The molecular formula of curtisian U (**4**) was established as C<sub>30</sub>H<sub>30</sub>O<sub>12</sub> by high resolution FAB-mass spectrometry providing a molecular ion peak at  $m/z$  605.1640 [ $M+Na$ ]<sup>+</sup> ( $\Delta + 0.5$  mmu). Its UV absorption maximum at 262 nm indicated the presence of an aromatic group, and its IR spectrum suggested the presence of hy-

droxyl (3445 cm<sup>-1</sup>) and aromatic (1650, 1560 cm<sup>-1</sup>) groups. The <sup>1</sup>H NMR spectrum in CD<sub>3</sub>OD exhibited signals due to a 1,4-disubstituted benzene at  $\delta$  7.07 and 6.82, a 3-hydroxybutyryl moiety at  $\delta$  4.00, 2.43, 2.28, and 1.04, and an acetyl methyl at  $\delta$  1.96. 3-Hydroxybutyryl and acetyl moieties were confirmed by COSY and HMBC correlations shown in Figure 2. Thirteen signals observed in the <sup>13</sup>C NMR spectrum suggested that compound **4** was a symmetrical structure with two 3-hydroxybutyryl and two acetyl sub-

**Table 2**<sup>1</sup>H and <sup>13</sup>C NMR spectral data for compounds **4** and **5** in CD<sub>3</sub>OD

No.	4		5	
	$\delta_C$	$\delta_H$	$\delta_C$	$\delta_H$
1,1''	123.4		123.3, 123.2	
2,6,2'',6''	132.0	7.07 (d, $J = 8.0$ ) <sup>a</sup>	132.0, 132.1	7.06, 7.08 (d, $J = 8.4$ )
3,5,3'',5''	116.2	6.82 (d, $J = 8.0$ )	116.1, 116.2	6.80, 6.81 (d, $J = 8.4$ )
4,4''	158.9		158.9	
1',4'	131.6		131.5, 131.6	
2',3',5',6'	140.7, 140.5		140.5, 140.6, 140.7	
1a	170.1		170.2	
2a	44.1	2.28, 2.43 (dd, $J = 6.4, 15.6$ )	44.0	2.31, 2.47 (dd, $J = 6.4, 15.6$ )
3a	65.1	4.00 (m)	65.0	3.97 (m)
4a	23.1	1.04 (d, $J = 6.0$ )	23.1	1.01 (d, $J = 6.4$ )
1b	169.7		170.2	
2b	20.2	1.96 (s)	44.0	2.31, 2.47 (dd, $J = 6.4, 15.6$ )
3b			65.0	3.97 (m)
4b			23.1	1.01 (d, $J = 6.4$ )
1c	170.1		171.5	
2c	44.1	2.28, 2.43 (dd, $J = 6.4, 15.6$ )	35.9	2.57 (t, $J = 7.2$ )
3c	65.1	4.00 (m)	31.2	2.71 (t, $J = 7.2$ )
4c	23.1	1.04 (d, $J = 6.0$ )	141.5	
5c,9c			129.3	7.06 (overlapped)
6c,8c			129.5	7.22 (t, $J = 8.0$ )
7c			127.3	7.14 (t, $J = 8.0$ )
1d	169.7		169.0	
2d	20.2	1.96 (s)	19.9	1.79 (s)

All spectra were recorded at 400 MHz for proton and at 100 MHz for carbon.

<sup>a</sup> Proton resonance multiplicity and coupling constant ( $J = \text{Hz}$ ) in parenthesis.

**Table 3**  
Free radical scavenging activity of curtisians (IC<sub>50</sub> value,  $\mu$ M)

Compounds	DPPH <sup>a</sup>	ABTS <sup>b</sup>	Superoxide <sup>c</sup>
Curtisian I	>500	60.41 $\pm$ 4.53	>500
Curtisian J	>500	13.45 $\pm$ 0.55	>500
Curtisian K	>500	11.30 $\pm$ 0.07	>500
Curtisian L	>500	18.64 $\pm$ 0.10	>500
Curtisian M	>500	8.15 $\pm$ 0.18	>500
Curtisian N	>500	5.50 $\pm$ 0.23	>500
Curtisian O	>500	7.11 $\pm$ 0.19	>500
Curtisian P	>500	6.44 $\pm$ 0.39	>500
Kynapcin-12	>500	8.77 $\pm$ 0.18	>500
Curtisian E	>500	>500	>500
Curtisian R (1)	>500	8.02 $\pm$ 0.28	>500
Curtisian S (2)	>500	8.16 $\pm$ 0.34	>500
Curtisian T (3)	>500	8.43 $\pm$ 0.29	>500
Curtisian U (4)	>500	>500	>500
Curtisian V (5)	>500	>500	>500
Trolox	33.00 $\pm$ 1.79	7.91 $\pm$ 0.05	>500
Caffeic acid	21.11 $\pm$ 1.22	5.37 $\pm$ 0.09	58.0 $\pm$ 4.3
BHA	82.97 $\pm$ 10.60	10.71 $\pm$ 0.09	>500

Results presented as the mean ( $n = 3$ )  $\pm$ SD.

<sup>a</sup>  $\alpha,\alpha$ -Diphenyl- $\beta$ -picrylhydrazyl.

<sup>b</sup> 2,2'-Azinobis-(3-ethylbenzothiazoline-6-sulfonic acid).

<sup>c</sup> Xanthin/xanthin oxidase.

stituents on the central aromatic ring of the *p*-terphenyl moiety.<sup>6</sup> Finally, the structure was determined by a NOESY spectrum, which displayed correlations between the methyl protons of the acetyl group and the methylene and oxymethine protons of the 3-hydroxybutyryl group (Fig. 1). These results indicated that two 3-hydroxybutyryl groups were linked to the C-2' and C-5' of the central aromatic ring, while two acetyl groups were attached to C-3' and C-6'. Therefore, the structure of **4** was determined to be a new *p*-terphenyl, as shown in Figure 1.

Curtisian V (**5**) was obtained as a dark brown powder and its molecular formula was established as C<sub>37</sub>H<sub>36</sub>O<sub>12</sub> by high resolution FAB-mass ( $m/z$  695.2094 [M+Na]<sup>+</sup>,  $\Delta = 1.1$  mmu). The UV absorption maximum (262 nm) and IR absorption bands (3445, 1651, and 1560 cm<sup>-1</sup>), similar to compound **4**, indicated that compound **5** might be a *p*-terphenyl with four substituents. The <sup>1</sup>H NMR spectrum in CD<sub>3</sub>OD revealed the presence of two *para*-hydroxy phenyls ( $\delta$  7.08, 7.06, 6.81, and 6.80), one phenyl ( $\delta$  7.22, 7.14, and 7.06), an acetyl methyl ( $\delta$  1.79), two methyls ( $\delta$  1.01), two methines ( $\delta$  3.97), two nonequivalent methylenes ( $\delta$  2.31 and 2.47), and two methylenes ( $\delta$  2.57 and 2.71) (Table 2). The presence of the two 3-hydroxybutyryl groups was established by HMBC correlations of H-2 and H-3 of the two 3-hydroxybutyryl moieties to the C-1, and a phenylbutyryl group was established by long-range correlations of H-2 of the phenylbutyryl to the C-1 and C-4. This NMR spectral data implied that **5** was composed of an acetyl, two 3-hydroxybutyryls, and a phenylbutyryl moiety. The substitution on the central aromatic ring of the *p*-terphenyl moiety was assigned by the NOESY spectrum, which exhibited NOE correlations between H-2 of the acetyl group and H-2 and H-3 of the phenylbutyryl group. This data indicated that the relative location of the acetyl group to the phenylbutyryl group was *ortho*. Thus, the structure of **5** was determined to be a new *p*-terphenyl, as shown in Figure 1.

Previously, the absolute configurations of the 3-hydroxybutyryl and 3-acetoxybutyryl substituents in known curtisians were reported to be *S* through saponification, methylation, and acetylation procedures.<sup>6,7</sup> From the co-occurrence of known curtisians, the absolute configurations of the 3-acetoxybutyryl in **3** and 3-hydroxybutyryls in **4** and **5** were proposed to be *S*.

### 3. Antioxidant activity

In order to evaluate the radical scavenging activity of isolated curtisians, the DPPH radical, ABTS (2,2'-azinobis(3-ethylbenzothiazoline-6-sulfonate)) radical, superoxide radical, and hydroxyl radical scavenging assay methods were employed. The DPPH, ABTS, and superoxide radical scavenging activities were defined as the amount of antioxidant necessary to decrease the initial radical concentration by 50% (IC<sub>50</sub>). All samples tested, except for curtisians E, U, and V, scavenged the ABTS radical but did not scavenge DPPH or the superoxide radical, as shown in Table 3. Curtisians M–P and R–T scavenged the ABTS radical as much as trolox and BHA (butylated hydroxyanisole), which are involved in a sequential reduction of ABTS radicals followed by trapping of these radicals.

The formation of hydroxyl radicals from the Fenton reaction between ferrous and hydrogen peroxide was measured using 2-deoxyribose oxidative degradation and plasmid DNA single strand breakage (SSB), respectively. Figure 2 shows a comparison among curtisians, classical antioxidants (trolox and BHA), and a traditionally used iron chelator (desferrioxamine, DFO) in preventing 2-deoxyribose degradation induced by ferrous and hydrogen peroxide. The principle of the assay is the quantification of the main 2-deoxyribose degradation product, malonaldehyde (MDA), by its condensation with TBA.<sup>11,12</sup> Curtisians E, K, M, N, and O, and kynapcin-12 were comparable to trolox and DFO at 100.0  $\mu$ M concentration, and were remarkably more active than BHA. The oxidative DNA damage mediated by iron was also evaluated using an in vitro technique, which proved to be a very sensitive indicator of DNA damage.<sup>13,14</sup> This assay allowed the quantification of a circular form of DNA generated by a single nick in a supercoiled plasmid, leading to DNA SSB. DFO was used as a positive control. As a result, 50.0  $\mu$ M of all curtisians isolated, kynapcin-12, and DFO were found to inhibit the DNA damage induced by 12.5  $\mu$ M iron and 0.25 mM H<sub>2</sub>O<sub>2</sub>, while BHA exhibited no activity and trolox showed marginal activity, as shown in Figure 3. These results suggest that curtisians may be useful as iron chelators or antioxidants against oxidative damage.

## 4. Experimental

### 4.1. General methods

Specific rotation was determined using a JASCO P-1020 polarimeter. High-resolution FAB-mass was taken on a JMS-700 JEOL mass spectrometer. UV and IR spectra were recorded on Shimadzu UV-300 and FT-IR Equinox 55 spectrometers, respectively. NMR spectra were obtained on a Varian UNITY Inova NMR spectrometer with <sup>1</sup>H NMR at 400 MHz and <sup>13</sup>C NMR at 100 MHz in CD<sub>3</sub>OD.

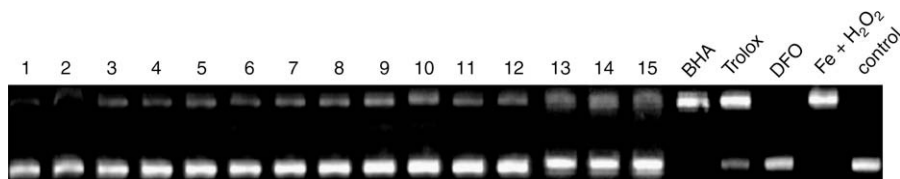


**Figure 3.** Protective effects of curtisians against plasmid DNA breakage by the Fenton reaction between ferrous and hydrogen peroxide. The number labels indicate: 1–8, curtisians I–P; 9, kynapcin-12; 10–12, curtisians R–T; 13, curtisian E; 14–15, curtisians U–V.



Chemical shifts are given in ppm ( $\delta$ ) with TMS as the internal standard.

## 4.2. Fungal material

The fruiting bodies of *P. curtisii* (dry weight 82.0 g) were collected at Odae National Parks in Korea. A voucher specimen was deposited in the herbarium of College of Environmental & Biore-source Sciences, Chonbuk National University.

## 4.3. Extraction and isolation

The fruiting bodies of *P. curtisii* were ground and extracted twice with MeOH at room temperature. After removal of the MeOH under reduced pressure, the resulting extract was partitioned between ethyl acetate and water. The ethyl acetate extract was chromatographed on a column of silica gel eluting with a gradient of increasing methanol (2–50%) in chloroform to afford active fractions. The fractions were collected, concentrated under reduced pressure, and subjected to a column of Sephadex LH-20 eluting with chloroform–methanol (1:1) to give two active fractions. One was further purified by  $C_{18}$  Sep-pak cartridge with a gradient of increasing methanol (25–100%) in water to give two fractions, and each fraction was followed by the reversed-phase preparative HPLC with 50% aqueous MeOH to give curtisian U (**4**, 4.2 mg) and curtisians I (41.0 mg), E (119.4 mg), and V (**5**, 27.6 mg), respectively. The other was divided into 5 fractions (fractions 1–5) by a column of Sephadex LH-20 eluting with methanol and a  $C_{18}$  Sep-pak cartridge with a gradient of increasing methanol (25–100%) in water. Fractions 1–5 were purified by reversed-phase preparative HPLC with a gradient of increasing methanol (40–60%) in water to give kynapcin-12 (8.7 mg) and curtisian L (1.2 mg) from fraction 1, curtisians N (30.0 mg), O (8.0 mg), M (4.9 mg), and K (22.7 mg) from fraction 2, curtisians T (**3**, 23.0 mg), P (23.4 mg), and J (4.7 mg) from fraction 3, curtisian S (**2**, 7.3 mg) from fraction 4, and curtisian R (**1**, 6.9 mg) from fraction 5.

### 4.3.1. Curtisian R (**1**)

Dark brown powder; UV (MeOH)  $\lambda_{\max}$  ( $\epsilon$ ) 262 (4.29) nm, 205 (4.72); IR (KBr)  $\nu_{\max}$  3402, 2958, 2839, 1674, 1651, 1018  $\text{cm}^{-1}$ ;  $^1\text{H}$  and  $^{13}\text{C}$  NMR data in Table 1; (+)-FABMS  $m/z$ : 591.2  $[\text{M}+\text{H}]^+$ ; (+)-HRFABMS  $m/z$ : 591.2062  $[\text{M}+\text{H}]^+$  (calcd for  $\text{C}_{36}\text{H}_{31}\text{O}_8$ , 591.2019).

### 4.3.2. Curtisian S (**2**)

Dark brown powder; UV (MeOH)  $\lambda_{\max}$  ( $\epsilon$ ) 262 (4.32), 203 (4.71) nm; IR (KBr)  $\nu_{\max}$  3400, 2951, 2839, 1651, 1018  $\text{cm}^{-1}$ ;  $^1\text{H}$  and  $^{13}\text{C}$  NMR data in Table 1; (+)-FABMS  $m/z$ : 529.3  $[\text{M}+\text{H}]^+$ ; (+)-HRFABMS  $m/z$ : 529.1874  $[\text{M}+\text{H}]^+$  (calcd for  $\text{C}_{31}\text{H}_{29}\text{O}_8$ , 529.1863).

### 4.3.3. Curtisian T (**3**)

Dark brown powder;  $[\alpha] -8.6$  (c 2.09, MeOH); UV (MeOH)  $\lambda_{\max}$  ( $\epsilon$ ) 263 (4.33), 229 (4.51), 202 (4.70) nm; IR (KBr)  $\nu_{\max}$  3400, 2950, 2830, 1701, 1651, 1022  $\text{cm}^{-1}$ ;  $^1\text{H}$  and  $^{13}\text{C}$  NMR data in Table 1; (+)-FABMS  $m/z$ : 559.2  $[\text{M}+\text{H}]^+$ ; (+)-HRFABMS  $m/z$ : 559.1567  $[\text{M}+\text{H}]^+$  (calcd for  $\text{C}_{31}\text{H}_{27}\text{O}_{10}$ , 559.1604).

### 4.3.4. Curtisian U (**4**)

Dark brown powder;  $[\alpha] -2.5$  (c 0.22, MeOH); UV (MeOH)  $\lambda_{\max}$  ( $\epsilon$ ) 268 (4.12), 203 (4.58) nm; IR (KBr)  $\nu_{\max}$  3445, 2369, 2342, 1700, 1650, 1560  $\text{cm}^{-1}$ ;  $^1\text{H}$  and  $^{13}\text{C}$  NMR data in Table 2; (+)-FABMS  $m/z$ : 583.2  $[\text{M}+\text{H}]^+$ ; (+)-HRFABMS  $m/z$ : 605.1640  $[\text{M}+\text{Na}]^+$  (calcd for  $\text{C}_{30}\text{H}_{31}\text{O}_{12}$ , 605.1635).

### 4.3.5. Curtisian V (**5**)

Dark brown powder;  $[\alpha] -42.5$  (c 2.00, MeOH); UV (MeOH)  $\lambda_{\max}$  ( $\epsilon$ ) 268 (4.14), 203 (4.64) nm; IR (KBr)  $\nu_{\max}$  3445, 2369, 2342, 1700,

1651  $\text{cm}^{-1}$ ;  $^1\text{H}$ - and  $^{13}\text{C}$  NMR data in Table 2; (+)-FABMS  $m/z$  673.2  $[\text{M}+\text{H}]^+$ ; (+)-HRFABMS  $m/z$  695.2094  $[\text{M}+\text{Na}]^+$  (calcd for  $\text{C}_{37}\text{H}_{36}\text{O}_{12}$ , 695.2105).

## 4.4. Antioxidant activity

Antioxidant activity was evaluated by measuring the free radical scavenging effects against DPPH radicals, ABTS radical cations, superoxide radical anions, and hydroxyl radicals.

### 4.4.1. DPPH (1,1-diphenyl-2-picrylhydrazyl) radical scavenging activity assay

The ability of the samples to scavenge DPPH radicals was determined by the reported method.<sup>15</sup> Five milliliters of each sample, along with positive controls (BHA, trolox, caffeic acid) prepared in methanol (0.08–10.0 mM), were combined with 95.0  $\mu\text{L}$  of 150.0  $\mu\text{M}$  methanolic DPPH in triplicate. Following incubation at room temperature for 30 min, the absorbance at 517 nm was read on a Molecular Devices Spectromax microplate reader (Sunnyvale, CA, USA).

### 4.4.2. ABTS [2,2'-azinobis(3-ethylbenzothiazoline-6-sulfonate)] radical cation decolorization assay

ABTS radical scavenging activity was carried out by using an ABTS radical cation decolorization assay with minor modifications.<sup>16</sup> ABTS was dissolved in water to a concentration of 7.0 mM. The ABTS radical was produced by reacting the ABTS stock solution with 2.45 mM potassium persulfate and allowing the mixture to stand in the dark for 12 h. After adding 95.0  $\mu\text{L}$  of the ABTS radical cation solution to 5.0  $\mu\text{L}$  of antioxidant compounds in methanol, the absorbance was measured by a microplate reader at 734 nm after mixing for 6 min.

### 4.4.3. Superoxide radical anion scavenging activity assay

Superoxide radical anion scavenging activity was evaluated by the xanthine/xanthine oxidase method.<sup>17</sup> In brief, each well of a 96-well plate contained 100.0  $\mu\text{L}$  of the following reagents: 50.0 mM potassium phosphate buffer (pH 7.8), 1.0 mM EDTA, 0.04 mM NBT (nitroblue tetrazolium), 0.18 mM xanthine, 250 mU/mL xanthine oxidase, and each concentration of samples was incubated for 30 min at 37 °C in the dark. The xanthine oxidase catalyzes the oxidation of xanthine to uric acid and superoxide, and the superoxide reduces NBT to blue formazan. The reduction of NBT to blue formazan was measured at 560 nm in a microplate reader.

### 4.4.4. DNA single strand breakage assay

Supercoiled DNA from pBR322 (Roche) was incubated for 30 min at 25 °C in 10.0 mM Tris–HCl buffer (pH 7.5) and mixed with 50.0  $\mu\text{M}$  samples, 0.25 mM  $\text{H}_2\text{O}_2$ , and 12.5  $\mu\text{M}$  ferric chloride. Reactions were performed on 0.2  $\mu\text{g}$  of DNA at a final volume of 20.0  $\mu\text{L}$  and stopped by adding 10  $\mu\text{L}$  of a stop solution (4.0 M urea, 50% sucrose, 50.0 mM EDTA, 0.1% bromophenol blue). Samples were electrophoresed in 1% agarose gel in TAE buffer (40.0 mM Tris acetate, 2.0 mM EDTA, 20.0 mM sodium acetate), and the gel was stained with ethidium bromide. Untreated plasmid DNA revealed a band corresponding to the intact, supercoiled DNA.

### 4.4.5. 2-Deoxyribose degradation assay

The reactions were started by addition of hydrogen peroxide (final concentration, 100.0  $\mu\text{M}$ ) to 0.5 mL of a solution containing 20.0 mM HEPES buffer (pH 7.2), 15.0 mM 2-deoxyribose, 100.0  $\mu\text{M}$   $\text{FeSO}_4$ , and 5.0  $\mu\text{L}$  of sample. Reactions were carried out for 45 min at 37 °C in a shaking incubator to ensure continuous flow of  $\text{O}_2$  into the tubes and were terminated by the addition of TCA (3.0 M)–HCl (2.0 N), 1:1 mixture (0.25 mL) followed by 0.25 mL of 0.67% thiobar-

bituric acid solution. After boiling for 10 min, the absorbance of the solution at 532 nm was recorded. Protection of 2-deoxyribose (% of control) was calculated as follows:  $[1 - (T-B)/(C-B)] \times 100$  (%), in which T, C, and B are absorbance values at 532 nm of the sample treatment, the control (without sample), and the blank (without FeSO<sub>4</sub> and H<sub>2</sub>O<sub>2</sub>), respectively.

### Acknowledgments

This work was supported by the Korea Research Foundation Grant (KRF-2006-532-F00001) from the Korean Government (MOEHRD) and a Grant from the BioGreen 21 Program (20080401-034-069) of the Rural Development Administration (RDA), Republic of Korea.

### References and notes

- Halliwell, B.; Gutteridge, J. M. C. *Free Radicals in Biology and Medicine*, 3rd ed.; Clarendon Press, Oxford University Press: London, 1999.
- Yoshida, Y.; Saito, Y.; Jones, L. S.; Shigeri, Y. *J. Biosci. Bioeng.* **2007**, *104*, 439.
- Pryor, W. A. *Free Radical Biol. Med.* **2000**, *28*, 141.
- Yun, B.-S.; Lee, I.-K.; Kim, J.-P.; Yoo, I.-D. *J. Antibiot.* **2000**, *53*, 114.
- Lee, I.-K.; Yun, B.-S.; Kim, J.-P.; Kim, W.-G.; Ryoo, I.-J.; Oh, S.; Kim, Y.-H.; Yoo, I.-D. *Planta Med.* **2003**, *69*, 513.
- Quang, D. N.; Hashimoto, T.; Nukada, M.; Yamamoto, I.; Tanaka, M.; Asakawa, Y. *Phytochemistry* **2003**, *64*, 649.
- Quang, D. N.; Hashimoto, T.; Nukada, M.; Yamamoto, I.; Tanaka, M.; Asakawa, Y. *Planta Med.* **2003**, *69*, 1063.
- Quang, D. N.; Hashimoto, T.; Nukada, M.; Yamamoto, I.; Tanaka, M.; Asakawa, Y. *Chem. Pharm. Bull.* **2003**, *51*, 1064.
- Lee, H. J.; Rhee, I. K.; Lee, K. B.; Yoo, I. D.; Song, K. S. *J. Antibiot.* **2000**, *53*, 714.
- Liu, J.-K. *Chem. Rev.* **2006**, *106*, 2209.
- Hermes-Lima, M.; Wang, E. M.; Schulman, H. M.; Storey, K. B.; Ponka, P. *Mol. Cell. Biochem.* **1994**, *137*, 65.
- Lopes, G. K. B.; Schulman, H. M.; Hermes-Lima, M. *Biochim. Biophys. Acta* **1999**, *1472*, 142.
- Su, M.; Yang, Y.; Yang, G. *FEBS Lett.* **2006**, *580*, 4136.
- Galey, J.-B.; Destree, O.; Dumats, J.; Genard, S.; Tachon, P. *J. Med. Chem.* **2000**, *43*, 1418.
- Blois, M. S. *Nature* **1958**, *181*, 1199.
- Re, R.; Pellegrini, N.; Proteggente, A.; Pannala, A.; Yang, M.; Rice-Evans, C. *Free Radical Biol. Med.* **1999**, *26*, 1231.
- Matsushige, K.; Basnet, P.; Kadota, S.; Namba, T. *J. Trad. Med.* **1996**, *13*, 217.